PNAS RESEARCH ARTICLE | NEUROSCIENCE

Gephyrin promotes autonomous assembly and synaptic localization of GABAergic postsynaptic components without presynaptic GABA release

Etta Carricaburu[a], Orion Benner[a], Scott R. Burlingham[a], Carolina Dos Santos Passos[a], Natalia Hobaugh[b], Charles H. Karr[a], and Soham Chanda[a,c,d,1]

Affiliations are included on p. 11.

Edited by John Rubenstein, University of California, San Francisco, CA; received August 30, 2023; accepted May 17, 2024

Synapses containing γ-aminobutyric acid (GABA) constitute the primary centers for inhibitory neurotransmission in our nervous system. It is unclear how these synaptic structures form and align their postsynaptic machineries with presynaptic terminals. Here, we monitored the cellular distribution of several GABAergic postsynaptic proteins in a purely glutamatergic neuronal culture derived from human stem cells, which virtually lacks any vesicular GABA release. We found that several $GABA_A$ receptor ($GABA_AR$) subunits, postsynaptic scaffolds, and major cell-adhesion molecules can reliably coaggregate and colocalize at even GABA-deficient subsynaptic domains, but remain physically segregated from glutamatergic counterparts. Genetic deletions of both Gephyrin and a Gephyrin-associated guanosine di- or triphosphate (GDP/GTP) exchange factor Collybistin severely disrupted the coassembly of these postsynaptic compositions and their proper apposition with presynaptic inputs. Gephyrin–$GABA_AR$ clusters, developed in the absence of GABA transmission, could be subsequently activated and even potentiated by delayed supply of vesicular GABA. Thus, molecular organization of GABAergic postsynapses can initiate via a GABA-independent but Gephyrin-dependent intrinsic mechanism.

neurotransmitter release | synapse formation | GABAergic synapse | Collybistin | Gephyrin

Significance

Impairment in synapse properties leads to a number of severe neurological disorders. However, even at basic cell biological level, it is not well understood how synaptic connections establish and properly align their pre- vs. postsynaptic specifications. To address this fundamental question, we examined the molecular mechanism of γ-aminobutyric acid (GABA) sensing postsynapse formation in stem cell –derived human neurons. We observed that major GABAergic postsynaptic components begin to self-assemble and properly align with presynaptic terminals, even in the complete absence of GABA signals. The scaffolding molecule Gephyrin played a critical role in organizing these "orphan" postsynaptic structures, which could be subsequently activated by a delayed supply of vesicular GABA. Our results highlight a transmitter-independent pathway that pioneers GABAergic postsynapse development.

γ-aminobutyric acid (GABA) is a major neurotransmitter that plays a critical inhibitory role in regulating the cellular excitability of neurons. GABA is biosynthesized by glutamate decarboxylase enzymes (i.e., GAD65 and GAD67), packaged into secretory vesicles by the GABA transporter (i.e., vGAT), released from presynaptic terminals, and activates ionotropic $GABA_A$ receptors ($GABA_ARs$) localized at the postsynaptic membranes. Efficient organization of GABAergic synapses requires an appropriate assembly of various pre- and postsynaptic elements, which in turn, ensure optimal alignment of $GABA_ARs$ with GABA release sites. However, the cell biological processes that help establish, maintain, and modulate these unique subsynaptic structures are not well understood.

Evidently, the postsynaptic interface of GABAergic synapses recruits and retains different proteins that affect their formation and/or maturation. Of these, the scaffolding molecule Gephyrin is an important component that self-aggregates beneath the cell membrane and anchors several factors involved in synapse development (1). Gephyrin produces a hexameric lattice via its intramolecular interactions, which supposedly binds to the intracellular loops of specific $GABA_AR$ α-subunits and essentially determines their synaptic concentrations (2–5), although Gephyrin-independent clustering of $GABA_ARs$ has also been reported (6).

In addition to $GABA_ARs$, Gephyrin displays affinity for the $GABA_AR$-associated protein (GABARAP; (7)), various cytoskeletal components [e.g., Dynein, G-actin, Profilin, and Mena; (8, 9)], a Rho family guanine nucleotide exchange factor (Rho-GEF) Collybistin [ARHGEF9; human homolog hPEM-2; (10, 11)], synaptic cell-adhesion molecule (CAM) Neuroligin-2 [NLGN2; (12, 13)], and peptidyl-prolyl isomerase NIMA-interacting protein 1 (Pin1) which catalyzes a cis-trans conformational switch in its substrates including NLGN2 (14). Hence, Gephyrin acts to integrate different molecular compositions of the GABAergic postsynapse that are vital for its function, and confers a unique structural identity to this complex which is considerably distinct from its glutamatergic counterpart.

Despite this existing knowledge of Gephyrin's molecular interactome (15), its functional impact on GABAergic synapse organization is yet to be fully reconciled. In mouse models, both constitutive and conditional knockouts (KOs), disease-associated mutations, and small hairpin RNA (shRNA) –mediated knockdown of Gephyrin caused an extensive loss of synaptic $GABA_ARs$ without altering glutamatergic synapses (2, 16, 17). However, another study has described a relatively moderate GABAergic phenotype in $Gephyrin^{KO}$ animals,

The authors declare no competing interest.

This article is a PNAS Direct Submission.

[1]To whom correspondence may be addressed. Email: soham.chanda@colostate.edu.

This article contains supporting information online at https://www.pnas.org/lookup/suppl/doi:10.1073/pnas.2315100121/-/DCSupplemental.

Published June 18, 2024.

which predominantly affected the Glycinergic synapses instead (18). Albeit a widespread expression pattern of Gephyrin in different regions of the human brain (19), its role in GABAergic synapse development has not yet been characterized in human neurons.

Moreover, it remains unclear how Gephyrin localizes at the subsynaptic domain and whether Gephyrin itself can organize the GABAergic postsynapse by intrinsic scaffolding properties or needs to be additionally coupled with synaptic activities. Interestingly, genetic deletions of the $GABA_AR$ complex markedly impaired Gephyrin aggregation (20). Furthermore, Gephyrin and $GABA_AR$ clusters were substantially decreased in several brain regions of Collybistin-deficient animals (21). $NLGN2^{KO}$ can similarly reduce Gephyrin assembly, although this phenotype was primarily restricted to the perisomatic regions without altering its dendritic abundance (12, 22). These crucial studies imply that depending on local microenvironments of subcellular compartments, molecular affinities between Gephyrin and multiple binding partners might enable postsynapse formation.

A parallel hypothesis suggests that GABA release from presynaptic terminals and activation of $GABA_ARs$ could be directly responsible for the recruitment of Gephyrin–$GABA_AR$ complex at postsynaptic membranes. In agreement with this theory, immature and developing GABAergic synapses often exhibit elevated vGAT levels that precedes Gephyrin enrichment (23). Chronic inhibition of synaptic activities by pharmacological agents can diminish, although does not fully eliminate, postsynaptic $GABA_AR$ assembly (24, 25). In addition, the decline of Gephyrin clustering in $GABA_AR^{KO}$ neurons could also be mediated by silencing GABAergic transmission (20). Perhaps the most convincing evidence for a GABA-dependent mechanism appears from rapid photolysis of "caged" GABA near dendritic branches, which facilitates local accumulation of Gephyrin (26). Nevertheless, it is unknown whether transmitter-induced mechanisms also operate at synapses and whether GABAergic postsynaptic machineries including Gephyrin cease to recognize synaptic inputs without adequate GABA signaling, and/or fail to preserve their exclusive molecular compositions that are unique from other synapse types.

More recently, we have shown that ectopic expressions of vGAT + GAD65 + GAD67 (termed as "V57" factors) can effectively produce GABA also in purely glutamatergic neurons and release it from their presynapses, which in turn, can generate fully functional GABAergic postsynapses both in vitro and in vivo (27). However, it was not explicitly assessed whether this induction of GABAergic activities was essentially triggered by i) GABA-mediated recruitment and de novo assembly of postsynaptic elements, or ii) functional activation and further potentiation of developing or already existing postsynaptic structures that can initially self-organize irrespective of presynaptic GABA signaling. In this current study, we set out to monitor postsynapse formation in the complete absence of GABAergic neurotransmission. Our findings underscore a cell-autonomous mechanism that guides the origination of human GABAergic postsynapses.

Results

GABAergic Postsynaptic Proteins Can Self-Aggregate Without Presynaptic GABA Release. To examine GABAergic postsynapse development in a system lacking GABAergic presynapses, we reprogrammed induced pluripotent stem (iPS) cells into human neurons by a single transcription factor, Neurogenin-2 [Ngn2; (28, 29)], and cocultured them with mouse primary astrocytes devoid of murine neurons (Fig. 1*A* and *SI Appendix*, Fig. S1*A*). At postinduction day 30, current-clamp recordings detected robust action-potential firing and the presence of voltage-gated Na^+/K^+ channels, indicating their functional maturation (*SI Appendix*, Fig. S1 *B* and *C*). Furthermore, coimmunostaining for dendritic MAP2 and presynaptic marker Synapsin confirmed efficient synapse formation (Fig. 1*B*). In accordance, voltage-clamp recordings also revealed prominent spontaneous postsynaptic currents (sPSCs; Fig. 1*C*). However, these sPSC events could be readily eliminated by acute bath applications of AMPA-receptor (AMPAR) and NMDA-receptor (NMDAR) inhibitors (i.e., CNQX + CPP) corroborating that Ngn2-induced neurons are predominantly glutamatergic and missing functional GABAergic synapses (Fig. 1*C*), consistent with previous studies (28, 30).

To determine whether the absence of GABAergic transmission is caused by a lack of pre- and/or postsynaptic machineries, we conducted western blot experiments. We observed that the neurons contained limited levels of presynaptic GAD65, GAD67, and vGAT, that are necessary for GABA synthesis and its vesicular release, but possessed major postsynaptic elements, e.g., $GABA_ARs$, NLGN2, or Gephyrin (Fig. 1 *D* and *E*). This offered us an optimal platform to evaluate their coassembly and synaptic association in a GABA-free cellular environment.

To visualize cellular localizations of these GABAergic postsynaptic components, we immunostained them individually. In a permeabilized state, antibodies against Gephyrin and an intracellular epitope of NLGN2 identified elaborate distribution of both proteins along the MAP2-positive dendrites (Fig. 1 *F* and *G*). Under a nonpermeable staining condition, $GABA_AR$ antibodies raised against extracellular epitopes also revealed their clustered pattern on the cell surface and pronounced association of various subunits (e.g., α2, α3, β1, β2) with the dendritic membrane (Fig. 1 *F* and *G* and *SI Appendix*, Fig. S2*A*). To further investigate whether these different postsynaptic molecules create discrete puncta separately from each other or effectively aggregate as colocalized objects, we labeled them in pairs (Fig. 1*H* and *SI Appendix*, Fig. S2*B*). We detected compelling spatial overlaps between Gephyrin vs. NLGN2, $GABA_AR$ α3 and γ2, but minimally with α2 subunit (Fig. 1 *I*–*K* and *SI Appendix*, Fig. S2*B*). Moreover, the sizes of NLGN2 and α3 puncta were considerably magnified when accumulated within Gephyrin signals (Fig. 1 *I* and *K*). Thus, several postsynaptic proteins can directly couple with Gephyrin in a GABA-independent manner.

Postsynaptic Machineries Successfully Align with GABA-Deficient Presynaptic Terminals. We wondered whether these self-organizing Gephyrin–$GABA_AR$ clusters integrate at subsynaptic domains or mistarget at extrasynaptic sites. To inspect that, we immunostained individual GABAergic postsynaptic markers along with presynaptic Synapsin. We noticed that considerable fractions of Gephyrin, NLGN2, and α3 puncta were heavily enriched at areas adjacent to Synapsin signals with enlarged volumes (Fig. 2 *A*–*C*). A similar enhancement was observed for $GABA_AR$ γ2 recruitment, especially at synapses containing Gephyrin (*SI Appendix*, Fig. S2*B*). The Synapsin signals, however, did not exhibit efficient colocalization with β-Dystroglycan, a postsynaptic CAM associated with α-Dystroglycan and Dystrophin complex that interacts with presynaptic Neurexins (NRXNs) and facilitates $GABA_AR$ accumulation at a subset of GABAergic synapses (31, 32) (Fig. 2*D*). Together, our results implied that these GABA-deficient subsynaptic regions can already dock and stabilize a number of selective proteins.

GABAergic Postsynaptic Structures Remain Segregated from Glutamatergic Postsynapses. Next, we asked whether these GABA-less postsynapses continue to maintain their unique organizational identity or aberrantly congregate with glutamatergic specifications. To this end, we immunolabeled day 30 neurons for glutamatergic postsynapse marker Homer and also detected prominent clusters that widely distributed along dendritic processes and preferentially

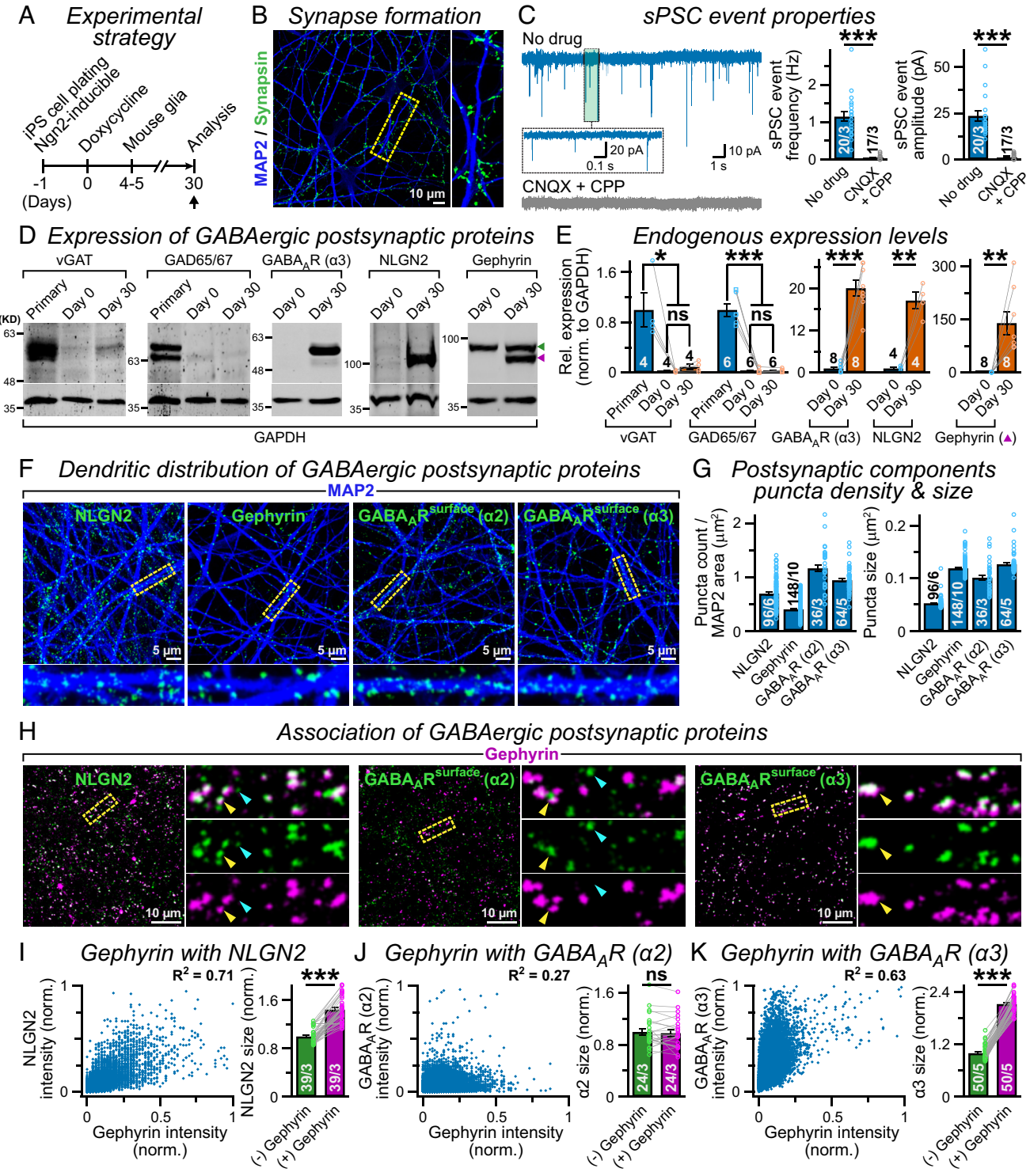

Fig. 1. GABAergic postsynaptic machineries self-organize without GABAergic neurotransmission. (*A*) Ngn2-inducible iPS cells (i.e., WTC-11 line) were reprogrammed into human neurons by doxycycline, cocultured with mouse glia, and analyzed at indicated time-points. (*B*) Representative image of neuronal cultures at postdifferentiation day 30, coimmunostained for MAP2 and Synapsin; *Inset* = boxed section further expanded to the *Right*. (*C*) Example sPSC traces (*Left*) before (No drug, *Top*; boxed area magnified) or after bath-applications of CNQX and CPP (*Bottom*); average frequency and amplitude (*Right*) of sPSC events. (*D* and *E*) Sample immunoblots (*D*) and average expression levels (*E*) of vGAT, GAD65/67, $GABA_AR$ α3, NLGN2, and Gephyrin (*Left* to *Right*) extracted from mouse hippocampal cultures (primary, positive control) vs. human iPS cells (Day 0, negative control) or iPS cell–derived neurons (Day 30); GAPDH = loading control. (*F* and *G*) Example images (*F*), average density and size (*G*) of NLGN2 or Gephyrin clusters immunostained under the permeabilized condition, or surface population of $GABA_ARs$ (α2 and α3 subunits) immunolabeled under the nonpermeabilized condition, distributed along MAP2-positive dendritic arbors. (*H*) Representative images of day 30 neurons immunostained for Gephyrin, paired with either NLGN2, $GABA_AR$ α2 or α3 (*Left* to *Right*). Boxed regions enlarged as merged views or individual channels. Arrowheads = signals that colocalize with (yellow) or distribute separately from (turquoise) Gephyrin puncta. (*I*–*K*) Relative intensities (*Left* panels, correlation plots with R-squared values) of NLGN2 (*I*), $GABA_AR$ α2 (*J*), and α3 (*K*) signals, with respect to coaggregated Gephyrin puncta, or their normalized cluster sizes (*Right* panels, bar graphs) when localized without (−) or with (+) a Gephyrin signal. All quantifications reflect means ± SEM. Statistics: Two-tailed Student's *t* test, with ***$P < 0.005$; **$P < 0.01$; *$P < 0.05$; ns = not significant ($P > 0.05$).

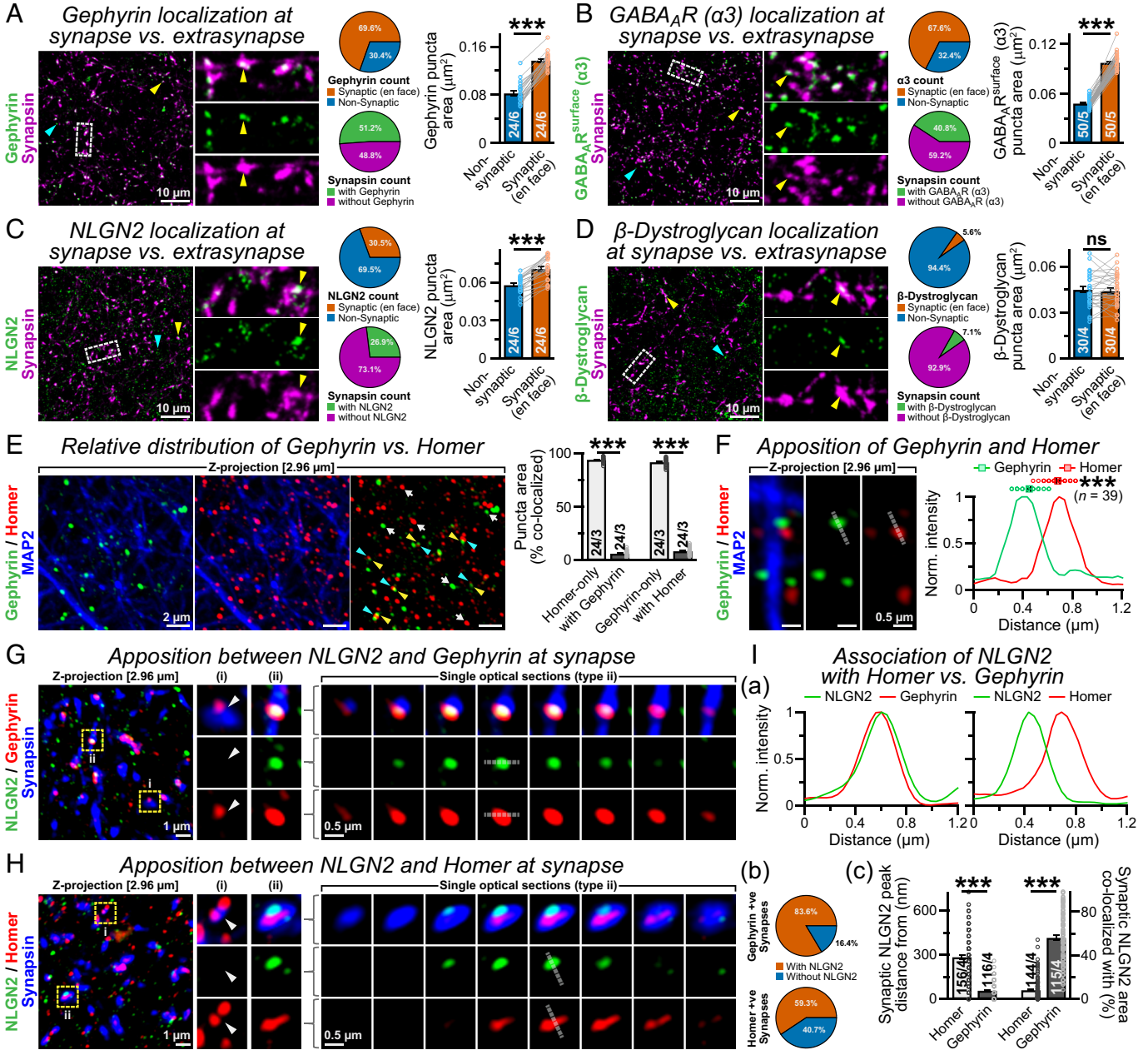

Fig. 2. Efficient alignment of the GABAergic postsynaptic complex with GABA-free presynaptic inputs. (*A–D*) Day 30 cultures immunostained for Synapsin, paired with Gephyrin (*A*), surface GABA$_A$R α3 (*B*), NLGN2 (*C*), or β-Dystroglycan (*D*). Representative images (*Left*) with boxed sections magnified, arrowheads = objects within (yellow) or outside (turquoise) Synapsin-positive areas; percentage (pie-charts, middle) of corresponding signals overlapped with Synapsin or vice versa; average puncta size (bar graphs, *Right*) of individual proteins clustered without (nonsynaptic) or with (synaptic, en face) Synapsin channel. (*E*) Coimmunostaining of Homer and Gephyrin with MAP2; merged views (*Left*, example images) and percentage of colocalization (*Right*, bar graphs). Superimposed image detects Homer (turquoise arrowheads) and Gephyrin (yellow arrowheads) puncta recruited at adjacent regions, or located independently of each other (white arrows). (*F*) Magnified super-resolution images (*Left*) and intensity profiles measured along the dashed lines (*Right*; with average distances between signal peaks) of Homer and Gephyrin puncta formed in close proximity on MAP2-positive dendritic segments. (*G*) Z-projected view (*Left*) of Synapsin, NLGN2, and Gephyrin colabeling; magnified boxes (*Middle*) depict Gephyrin puncta associated with synapses in the absence (type i, arrowheads) or presence (type ii) of a corecruited NLGN2 signal; single optical sections (*Right*) of type ii synapse. (*H*) Same as (*G*), except a pair of subsynaptic Homer and NLGN2 signals. (*I*) Normalized intensity profiles (*a*) of NLGN2 together with Gephyrin (*Left*) vs. Homer (*Right*), measured across dashed lines in panels (*G*) and (*H*); fractions (*b*, pie-charts) of Gephyrin- or Homer-positive subsynaptic domains that also possess NLGN2 signals; bar graphs (*c*) provide average peak distance (*Left*) or percentage of co-occupied territories (*Right*) between NLGN2 vs. Homer or Gephyrin clusters. Summary graphs represent means ± SEM. Statistics: Two-tailed, paired (panels *A–D*) or unpaired (*E*, *F*, and *I*), Student's *t* test, with ***$P < 0.005$; ns = not significant ($P > 0.05$).

accumulated near presynaptic terminals (*SI Appendix*, Fig. S2 *C* and *D*). The Homer signals also substantially colocalized with PSD-95, another authentic glutamatergic postsynapse marker (*SI Appendix*, Fig. S2*E*). Nevertheless, when labeled together with Gephyrin, the vast majority of Homer puncta illustrated minimal association and remained spatially segregated (Fig. 2*E*). A limited correlation was observed also among Gephyrin and PSD-95, as well as GABA$_A$R α3 and AMPAR GluA2 (*SI Appendix*, Fig. S2 *E* and *F*). Thus, GABAergic postsynaptic complexes do not share the same physical space with their glutamatergic counterparts.

We noticed that despite this spatial separation, Gephyrin and Homer puncta were occasionally positioned in close proximity to each other (Fig. 2*F*). To probe whether GABAergic postsynaptic elements continue to retain their compositional specificity even when located proximally to glutamatergic postsynapses, we immunolabeled the cells for NLGN2 and Synapsin in combination with

Gephyrin vs. Homer and performed super-resolution microscopy. We found that Gephyrin but not Homer signals were broadly colocalized with synaptic NLGN2 at single optical planes (Fig. 2 *G* and *H*). Compared to these well-aligned Gephyrin–NLGN2 clusters, the majority of Homer puncta remained sufficiently distant and shared negligible territory with adjacent NLGN2 signals (Fig. 2*I*), supporting the notion that GABAergic postsynaptic elements can maintain specificity and couple with correct partners, even in the absence of GABA.

Basal Synaptic Activities Are Not Necessary for the GABAergic Postsynapse Assembly. Although Ngn2 neurons did not show any measurable GABAergic transmission, we questioned whether GABA receptors could still be activated and modulated via a tonic, residual GABA release from non-neuronal sources, e.g., cocultured astrocytes (33, 34), beyond our detection limit. To assure that, we incubated the neurons with both $GABA_AR$ and $GABA_B$ receptor ($GABA_BR$) antagonists [Picrotoxin (PTX) and CGP55845 (CGP), respectively] immediately after differentiation, half-exchanged the media with drugs every 48 to 72 h, and analyzed them at different developmental time points. Between days 7 and 28, as the cells matured, they exhibited a progressive rise in the expression level and dendritic distribution of Synapsin, Gephyrin, and α3 (Fig. 3 *A* and *B*). Chronic treatments with GABA receptor blockers did not significantly affect synaptogenesis, density or size of Gephyrin–α3 clusters (Fig. 3 *A* and *B*). Moreover, co-localization among Synapsin, Gephyrin, and α3 puncta continued to grow substantially over time and stayed unaffected by drug applications (Fig. 3 *A* and *C*). Hence, synaptic enrichment of Gephyrin–$GABA_A$Rs was not dependent on any basal GABA signaling.

Furthermore, prolonged exposure to exogenous GABA in the culture media, which stimulates both synaptic and nonsynaptic receptors, caused a progressive loss of $GABA_AR$ clusters from synapses in a dose-dependent manner, without considerably altering their Gephyrin content (*SI Appendix*, Fig. S3 *A* and *B*). These findings further supported the idea that a global activation of $GABA_A$Rs cannot lead to their synaptic enrichment.

To address whether basal glutamatergic activities of Ngn2 neurons can potentially contribute to GABAergic postsynapse formation via heterosynaptic pathways, we similarly incubated them in CNQX + CPP (Fig. 1*C*). Long-term suppression of glutamatergic activities enhanced the size of Synapsin-positive presynaptic terminals and postsynaptic accumulation of glutamatergic specifications, e.g., Homer and GLUA2-AMPARs, purportedly via homeostatic mechanisms (Fig. 3 *D* and *E* and *SI Appendix*, Fig. S3 *C* and *D*). However, albeit a minor reduction in synaptic Gephyrin level, we failed to notice any major impairments in Gephyrin and $GABA_AR$ α3 clusters or their coassembly (Fig. 3 *D*–*F*). In sum, nascent GABAergic complexes can self-aggregate and begin to associate with subsynaptic domains, regardless of activities.

The Gephyrin Scaffold Enables the Subsynaptic Recruitment of $GABA_A$Rs Without GABA. We next wondered whether postsynaptic enrichment of GABAergic machineries was primarily mediated via an intrinsic, cell-autonomous mechanism. The steady presence of Gephyrin in these structures made us curious about its expression pattern during neurogenesis, and functional contribution at GABA-free postsynapses. We performed western blots for Gephyrin at multiple stages of neural differentiation and maturation and noticed a gradual change in its variant profile (Fig. 4 *A* and *B* and *SI Appendix*, Fig. S4*F*). In day 30 neurons, a considerable amount of Gephyrin was found to be processed in the cell bodies, which extensively trafficked at bona fine postsynapses of different sizes, formed on both soma and dendritic branches (Fig. 4*C*).

To test the hypothesis of Gephyrin-dependent scaffolding, we disrupted its endogenous loci in iPS cells using CRISPR-Cas9 and reprogrammed them into neurons by Ngn2 induction (*SI Appendix*, Fig. S4 *A* and *B*). These genetic manipulations did not affect the pluripotency properties of iPS cells and produced an isogenic line with truncated genome encompassing its guide RNA (gRNA) target (*SI Appendix*, Fig. S4 *C*–*E*). Immunoblot assays revealed complete loss of Gephyrin expression indicating a successful gene targeting and significant reduction in $GABA_AR$ α3 without affecting NLGN2 protein levels (Fig. 4*D* and *SI Appendix*, Fig. S4*F*).

Immunostaining of Gephyrin^{KO} neurons at day 30 confirmed depletion of Gephyrin clusters along dendrites (Fig. 4 *E* and *F*). Gephyrin^{KO} cells did not exhibit any impact on presynaptic Synaptotagmin-1 (Syt1) puncta, indicating a normal synaptogenesis process, but decreased the density and size of NLGN2 cluster and its subsynaptic levels (Fig. 4 *G* and *H*). Similar to Syt1, another presynaptic marker Synapsin or glutamatergic postsynaptic scaffold PSD-95 also remained unaffected in Gephyrin^{KO} neurons (Fig. 4 *I* and *J* and *SI Appendix*, Fig. S4*G*). Gephyrin deletion, however, virtually eliminated the submembrane aggregations of $GABA_AR$ α3 and its association with presynaptic terminals (Fig. 4 *I*–*K*). Therefore, the Gephyrin scaffold assists in the organization of the NLGN2–$GABA_AR$ complex, even at GABA-free postsynaptic compartments.

Collybistin Promotes Gephyrin–$GABA_AR$-NLGN2 Aggregation Irrespective of GABA Signal. In rodent models, Collybistin is known to modulate the formation and maintenance of Gephyrin clusters at several GABAergic postsynapses (10, 11). To probe whether similar mechanisms operate at human postsynapses, we knocked out its human analog hPEM-2 from iPS cells using the CRISPR-Cas9 method, which removed a significant portion from its genomic locus in X chromosome and created premature stop codons (*SI Appendix*, Fig. S4 *A*–*E*). We could not directly measure hPEM-2 protein level due to lack of reliable and commercially available antibody, but our RT-PCR assays from neurons reprogrammed from hPEM-2^{KO} iPS cells also illustrated definite loss of hPEM-2 mRNA segments, especially with primers designed against the Cas9-targeted genomic loci (Fig. 5*A*).

Western blots from hPEM-2^{KO} neurons did not demonstrate any significant change in Gephyrin, NLGN2, and $GABA_AR$ α3 protein content (Fig. 5*B*). However, relative to the wild-type (WT) condition, hPEM-2^{KO} neurons depicted a substantial reduction in the number and size of Gephyrin puncta distributed along the dendritic arbors, without affecting PSD-95 (Fig. 5 *C* and *D* and *SI Appendix*, Fig. S4*G*). hPEM-2 deletion also triggered major impairments in both NLGN2 and α3 clusterings, suggesting a defect in their ability to congregate, with only minor effect on Synapsin puncta (Fig. 5 *E* and *F*). To further examine synaptic targeting of Gephyrin, NLGN2, and α3, we costained them paired with Synapsin antibody (Fig. 5*G*). Once again, hPEM-2^{KO} neurons displayed obvious deficiencies in Gephyrin, NLGN2, or surface α3 signals that aggregate with each other and adequately assemble at subsynaptic domains (Fig. 5*H*). In sum, Gephyrin-mediated coalition of GABAergic postsynaptic machineries initiates via a Collybistin (or human hPEM-2) -dependent canonical mechanism that can sufficiently engage in GABA-free cellular environment.

The GABAergic Postsynaptic Complex Can Be Activated by Delayed Supply of Vesicular GABA. Because major GABAergic postsynaptic machineries already self-assembled without GABA signals and aligned properly with presynaptic inputs, we inquired whether those contained vesicular release machineries. Immunostainings

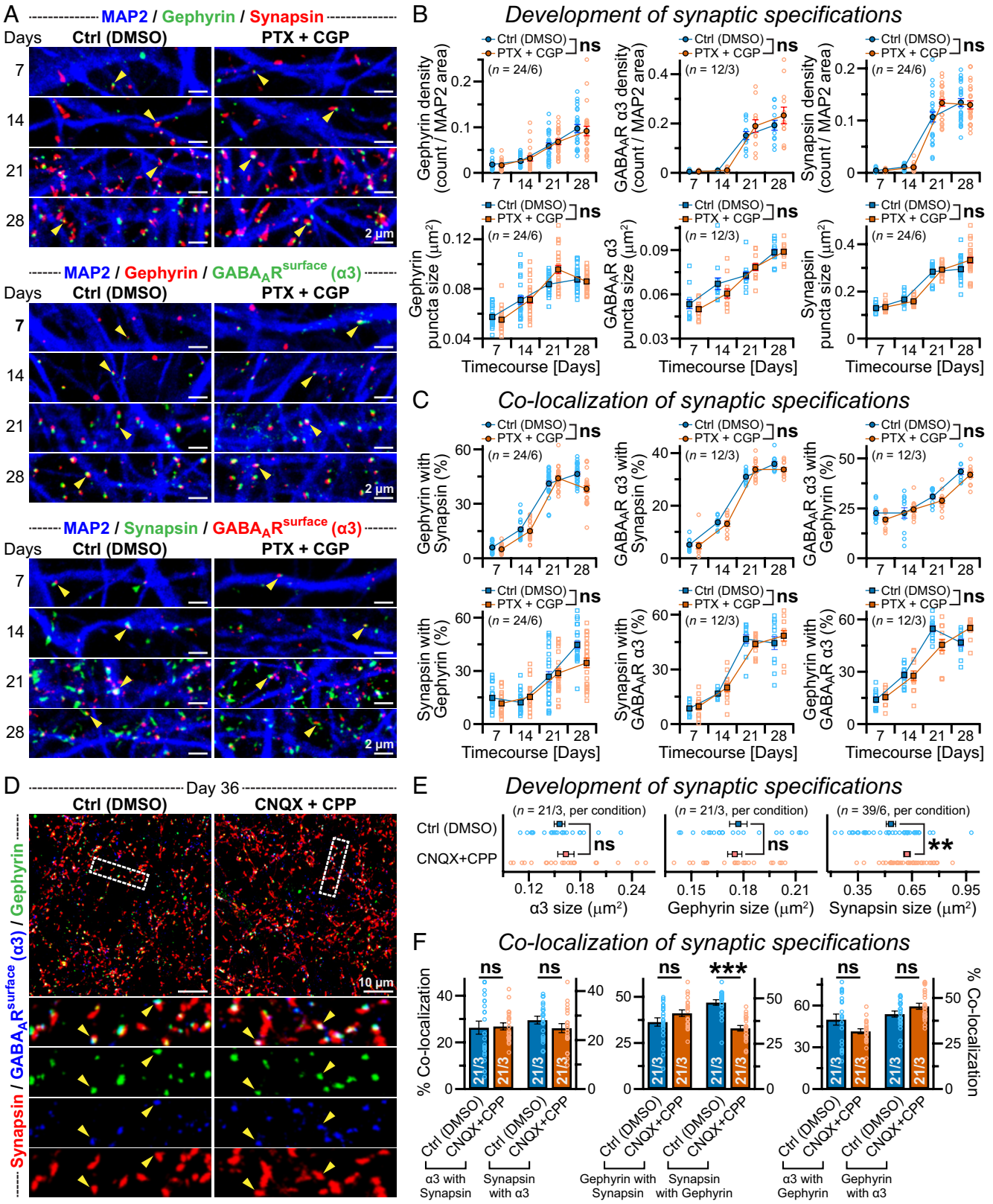

Fig. 3. Development of GABAergic postsynaptic structures in pharmacologically silenced neurons. (*A–C*) Sample images of Gephyrin, Synapsin, and surface GABA$_A$R α3 puncta (*A*) formed along MAP2-positive dendritic branches of human neurons at postinduction days 7, 14, 21, and 28 (arrowheads, *Top* to *Bottom* rows), their average density and size (*B*), or Mander's coefficients of colocalization (*C*), when continuously treated with either PTX (100 µM) + CGP (10 µM) or equal volume of DMSO (control, Ctrl), from day 4 to 5 to day 28. (*D–F*) Similar to (*A–C*), except when the cultures were exposed to 100 µM CNQX + 50 µM CPP, or DMSO (Ctrl), from day 4 to 5 to day 36. Sample images (*D*) with boxed regions magnified, and respective merged views split between individual channels; arrows = prominent colocalization. Average sizes of Gephyrin, Synapsin, or α3 puncta (*E*), and their relative degrees of association (*F*). Average values represent means ± SEM. Statistics: Two-way ANOVA (*B* and *C*), or two-tailed, unpaired (*E* and *F*), Student's *t* test (***$P < 0.005$; **$P < 0.01$; ns = not significant, $P > 0.05$).

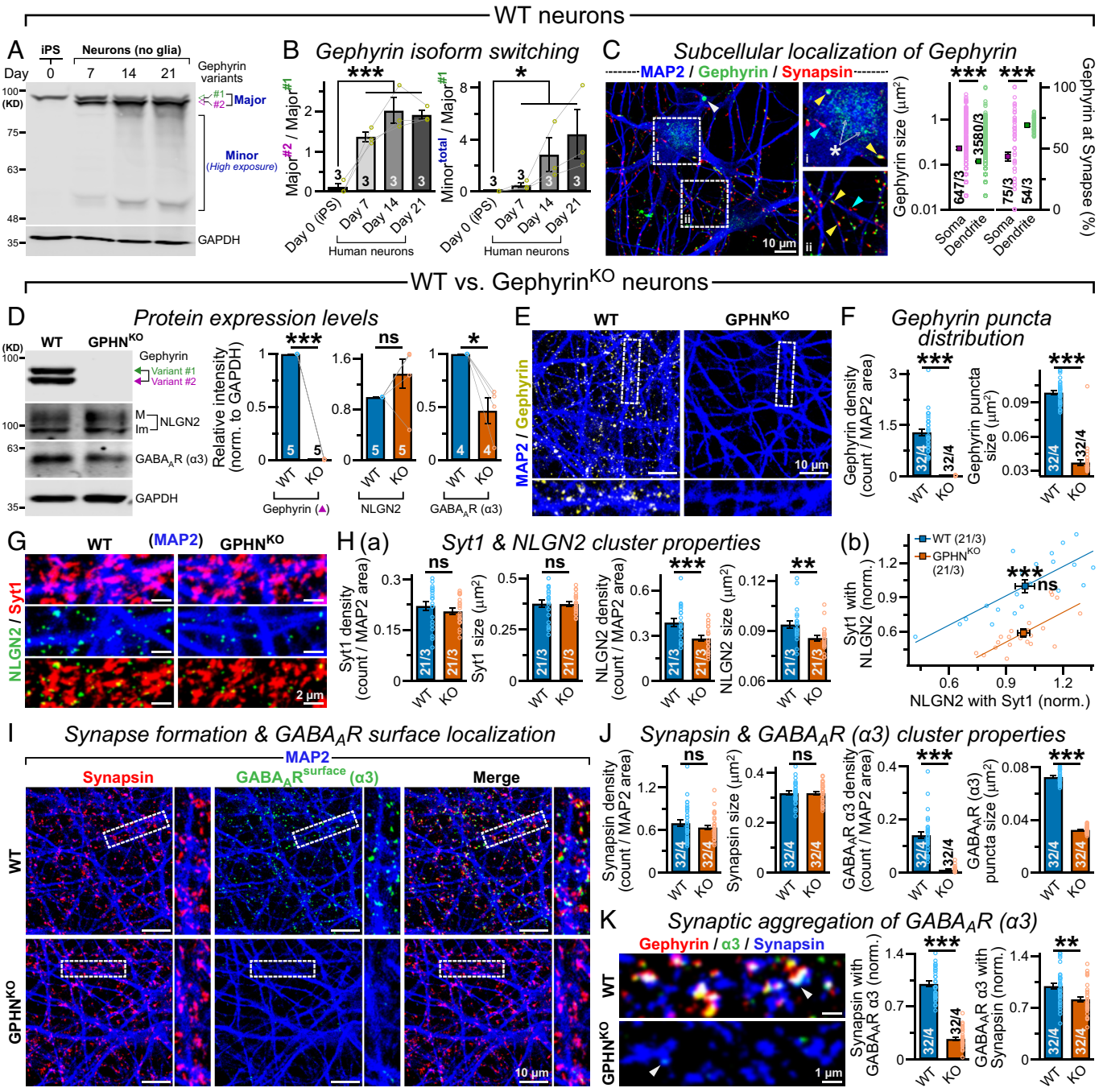

Fig. 4. Gephyrin-dependent enrichment of functionally inactive $GABA_ARs$ at subsynaptic domains. (*A* and *B*) Sample immunoblot (*A*) and normalized expression values (*B*) of endogenous Gephyrin extracted from WT iPS cells at day 0, or day 7, 14, and 21 human neurons, in the absence of mouse glia; two major (arrows, high molecular-weight) and multiple minor (bracket, lower molecular-weight) bands denote Gephyrin variants and/or degradation products (*SI Appendix*, Fig. S4*F*); GAPDH = loading control. (*C*) Representative images (*Left*; *Insets* = boxed areas magnified) and average size or synaptic association (*Right*) of Gephyrin puncta formed in the cell body (*i*) vs. dendritic segments (*ii*) of day 30 neurons. Arrows point at Gephyrin clusters lacking synaptic terminals (white), synaptic terminals lacking Gephyrin (cyan), or when both appose each other (yellow); asterisk = Gephyrin in the soma, potentially undergoing intracellular processing. (*D*) Example immunoblots (*Left*) and normalized expressions (*Right*) of endogenous Gephyrin (arrowheads = splice variants, green and magenta), maturely (M) vs. immaturely (Im) glycosylated NLGN2, and $GABA_AR$ α3, for WT vs. Gephyrin KO ($GPHN^{KO}$) neurons at day 7; GAPDH = loading control. (*E* and *F*) Representative images (*E*) and average density or size (*F*) of Gephyrin clusters formed on MAP2-labeled dendrites of WT vs. $GPHN^{KO}$ neurons at day 30. (*G* and *H*) Sample images (*G*) of MAP2-labeled dendrites immunostained for Syt1 and NLGN2, their average puncta density or size (*H*, panel *a*), and relative association with one another (*H*, panel *b*; data points fit with straight lines and compared along both x- and y-axis). (*I* and *J*) Sample images (*I*) of neurons immunolabeled for MAP2, Synapsin, and surface population of $GABA_ARs$ (α3); *Insets* = boxed sections expanded. Average density and size (*J*) of Synapsin (*Left*) or α3 (*Right*) puncta. (*K*) Example images (*Left*) of dendritic regions coimmunostained for Gephyrin, Synapsin, and $GABA_AR$ α3. Arrowheads point at α3 puncta essentially recruited at Gephyrin-positive synapses. Bar graphs (*Right*) report coefficients of colocalization between Synapsin and α3 objects. Summary plots are means ± SEM. Statistics: Two-tailed, paired (*B* and *D*, for western blot) or unpaired (*C* and *E*–*K*, for imaging), Student's *t* test, with ***$P < 0.005$; **$P < 0.01$; *$P < 0.05$; ns = not significant, $P > 0.05$.

for active-zone marker Bassoon or synaptic vesicle protein SV2 revealed that a sizable fraction of both Gephyrin and γ2 $GABA_AR$ puncta were indeed prepositioned across the presynaptic terminals containing vesicular release sites (*SI Appendix*, Fig. S5 *A*–*D*).

We therefore inquired whether these preexisting postsynaptic modules could be functionally stimulated post hoc by deferred GABA release from presynapse. To assess this possibility, we infected the day 30 neurons with lentiviruses encoding either a

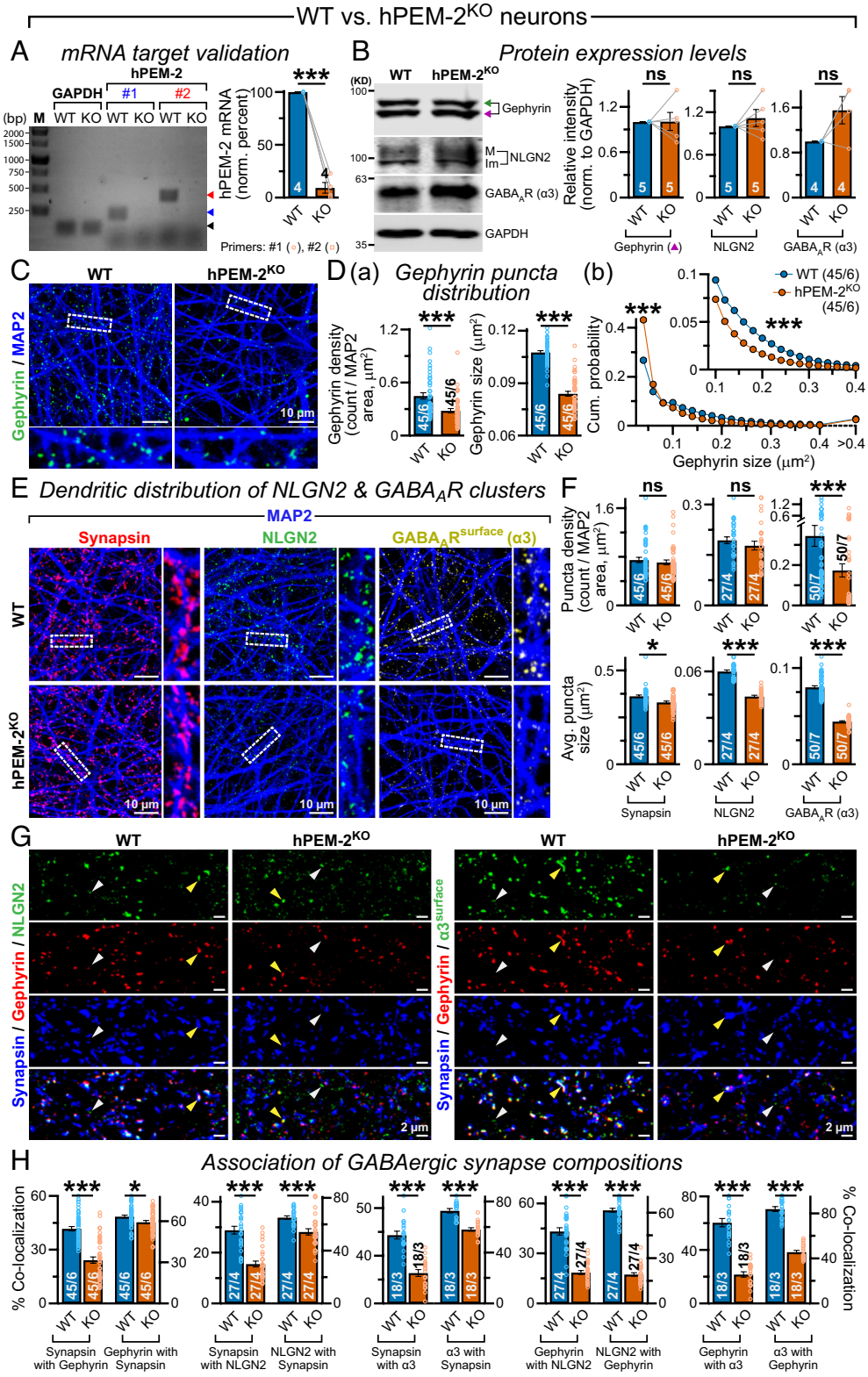

Fig. 5. Collybistin modulates the assembly of Gephyrin scaffolds without presynaptic GABA signals. (*A*) An agarose-gel (*Left*; M = DNA ladder) containing RT-PCR products; normalized mRNA expression (*Right*) of GAPDH and Collybistin (hPEM-2) in WT vs. hPEM-2^{KO} neurons at day 7. Arrowheads = predicted bands from two separate hPEM-2 primer sets (red and blue, see *SI Appendix*), or GAPDH product (black). (*B*) Example western blots (*Left*) and normalized expressions (*Right*) of Gephyrin (arrows, green and magenta), NLGN2 (M = mature, Im = immature), and $GABA_AR$ α3, at postinduction day 7; GAPDH = loading control. (*C* and *D*) Representative images (*C*) of day 30 neurons, coimmunostained for Gephyrin and MAP2. Morphological properties of Gephyrin puncta (*D*), in terms of density and cluster size (*a*), or cumulative distributions of puncta size binned by 0.02 μm^2 increment, further magnified in the *Inset* (*b*). (*E* and *F*) Example images (*E*) of WT (*Top*) vs. hPEM-2^{KO} (*Bottom*) neurons coimmunolabeled for indicated markers; *Insets* = expanded views. Average parameters (*F*) of Synapsin (*Left*), NLGN2 (*Middle*), and α3 (*Right*) signals, presented as their densities (*Top*) or cluster size (*Bottom*). (*G* and *H*) Sample images (*G*) depict dendritic regions of WT vs. hPEM-2^{KO} neurons coimmunostained for Synapsin and Gephyrin, in combinations with either NLGN2 (*Left* panels) or surface population of $GABA_AR$ α3 (*Right* panels); arrowheads indicate Gephyrin-positive synapses with (yellow) or without (white) NLGN2 or α3 objects. Mander's coefficients of colocalization (*H*) between Synapsin, Gephyrin, NLGN2, and α3. Average data are presented as means ± SEM. Statistics: Two-way ANOVA (cumulative plot, Db), or two-tailed, paired (*A* and *B*) or unpaired (Da and *E*–*H*), Student's *t* test (bar graphs), with ***$P < 0.005$; *$P < 0.05$; ns = not significant ($P > 0.05$).

control vector or all V57 factors combined, and subsequently analyzed them after an additional 21 d (Fig. 6*A*). Compared to the control condition, these V57-transduced neurons displayed robust expressions of both vGAT and GAD65/67 proteins that distributed elaborately at presynaptic terminals, without affecting their morphologies (Fig. 6 *B* and *C* and *SI Appendix*, Fig. S5*F*). Nearly all neurons in the V57 condition also synthesized high levels of GABA, which corroborated with the enzymatic actions of exogenous GADs (*SI Appendix*, Fig. S5*E*). Exogenous vGAT proteins also occupied a sizable fraction of the Synapsin-positive total presynapses but displayed only minor overlap with endogenous vGLUT-labeled glutamatergic terminals, emphasizing their mostly independent distributions (*SI Appendix*, Fig. S5 *G–I*), similar to the spatial segregation of their respective postsynaptic components (see Fig. 2 and *SI Appendix*, Fig. S2).

Our voltage-clamp recordings from day 51 control neurons revealed recurrent sPSCs with fast τ-decays that could be readily abolished by bath application of CNQX, again validating their purely glutamatergic identities (Fig. 6 *D* and *E*). The V57 condition, however, produced heterogeneous sPSC events comprising a mixture of either fast or slow τ-decay kinetics (*SI Appendix*, Fig. S5*J*). The slower sPSCs, in particular, could not be prevented by CNQX but acute treatment of PTX, suggesting a successful activation of postsynaptic $GABA_A$Rs by delayed supply of vesicular GABA (Fig. 6 *D* and *E*). Thus, self-organizing GABAergic postsynaptic structures could be functionally stimulated by de novo biosynthesis and ectopic release of presynaptic GABA.

Gephyrin and Collybistin Support the Functional Activation of GABAergic Postsynapses. To explore whether GABA transmission can influence the morphological properties of corresponding postsynaptic structures, we coimmunostained the cells with NLGN2 and vGAT antibodies. We noticed that deferred transduction of V57 factors caused a minor increase in NLGN2 puncta size without changing its density (Fig. 6 *F* and *G*). In the V57 condition, however, a large fraction of postsynaptic NLGN2 clusters were found to be aligned with presynaptic vGAT signals (Fig. 6 *F* and *H*). Similarly, delayed GABA release also triggered a significant but modest rise in Gephyrin density without affecting its cluster size (Fig. 6 *I* and *J*). Nevertheless, in the V57 condition, we detected prominent colocalization among GAD65/67 and Gephyrin signals (Fig. 6 *I* and *K*). Delayed V57 transduction did not significantly alter the positions of a few Gephyrin puncta that were mistargeted to vGLUT terminals, but substantially augmented their association with vGAT terminals (*SI Appendix*, Fig. S5*I*). Hence, vesicular GABA supply can further modulate preexisting GABAergic postsynaptic structures.

To verify whether Gephyrin aggregation was necessary for delayed activation of $GABA_A$Rs, we subsequently transduced both $Gephyrin^{KO}$ and $hPEM\text{-}2^{KO}$ neurons with V57 factors on day 30 and monitored the apposition of $GABA_A$R α3 with vGAT-positive puncta on day 51 (Fig. 6*A*). With respect to WT neurons, the KO conditions did not exhibit any significant difference in exogenous vGAT levels, suggesting comparable transgene expression (Fig. 6*L*). Both $hPEM\text{-}2^{KO}$ and $Gephyrin^{KO}$ cells, however, displayed profound reduction in their ability to recruit $GABA_A$Rs near the vGAT-positive terminals (Fig. 6*L*). When vesicular GABA was released by presynaptic stimulation, the WT neurons produced robust and reliable inhibitory PSCs (Fig. 6*M*). Amplitudes of these evoked PSCs were considerably attenuated in $hPEM\text{-}2^{KO}$, and virtually eliminated for $Gephyrin^{KO}$ neurons (Fig. 6*M*). These results suggest that dysregulation of Gephyrin can lead to severe deficit in the autonomous assembly of GABAergic postsynaptic machineries and their subsequent functional activation by presynaptic GABA release.

Discussion

Synapse assembly requires accurate alignment of presynaptic release sites with postsynaptic receptors. How neurons accomplish this precise structural configuration across trans-synaptic space is not understood. Sensory deprivation and pharmacological inhibition of overall activities were shown to affect cellular morphology and alter synaptogenesis by impaired axonal innervation (35–38). These results infer that transmitter release may instruct synapse formation. Nevertheless, acute silencing of transmitter release by genetic manipulations does not inhibit the initiation of synaptic contacts but instead impacts their long-term maintenance (39–45). Therefore, cell-autonomous mechanisms could also potentially contribute to the proper localization and unique distribution of synaptic elements, irrespective of neurotransmitter signals. Here, we provide additional evidence in support of this second model by elucidating the key factors that guide GABAergic postsynapse development without presynaptic GABA.

We observed that several GABAergic postsynaptic proteins, e.g., Gephyrin, NLGN2, $GABA_A$R α/β/γ subunits, can adequately distribute along the dendritic branches of human neurons without GABAergic activities, and congregate at subsynaptic domains lacking GABA (Figs. 1 and 2 and *SI Appendix*, Fig. S2). These results are in agreement with previous reports from rodent neurons grown as autaptic microisland cultures, or *Caenorhabditis elegans* neuromuscular junctions, which also detected efficient $GABA_A$R apposition with GABA-free inputs (46, 47). Moreover, a recent study demonstrated that synaptic $GABA_A$R nanodomains continue to develop despite global disruption of neurotransmitter release by tetanus neurotoxin (TeNT) (48). Based on current findings, we conclude that this fundamental principle of synapse organization is commonly shared across multiple species, and operates similarly in human cellular environment.

Of note, Ngn2 neurons produced an extensive number of Synapsin, Syt1, and SV2-positive synaptic terminals with Bassoon-containing active-zone machineries, but only a fraction of them possessed glutamatergic vGLUT signals, indicating the probable existence of silent presynapses with transmitter-free empty vesicles (Figs. 1 and 2 and *SI Appendix*, Fig. S5). In the absence of GABA, GABAergic postsynaptic components were localized indiscriminately at all synapses, with a minor fraction even mistargeted to vGLUT-labeled glutamatergic terminals (*SI Appendix*, Fig. S5), as similarly observed in the rodent system (46, 49). After V57 transduction, many of these endogenous Gephyrin–NLGN2–$GABA_A$R clusters began to appose presynaptic terminals that now contained exogenous vGAT and GAD65/67, triggering functional GABAergic activities (Fig. 6 and *SI Appendix*, Figs. S5 and S6).

In addition to prolonged incubation with $GABA_A$R and $GABA_B$R antagonists, which excluded the possible contribution of any residual GABA receptor activities from nonsynaptic sources, a pharmacological silencing of glutamatergic AMPAR and NMDAR also failed to suppress GABAergic postsynapse formation (Fig. 3 and *SI Appendix*, Fig. S3). Taken together, our results suggest that global synaptic activities including GABA release itself could be largely dispensable for the initial arrangement of GABAergic postsynaptic elements. An identical phenomenon was described for glutamatergic postsynapse development, which could also originate independently of glutamate transmission, when vesicular release was broadly interrupted by TeNT, or KOs of Ca^{2+} channels and Munc13/18 isoforms (39–45).

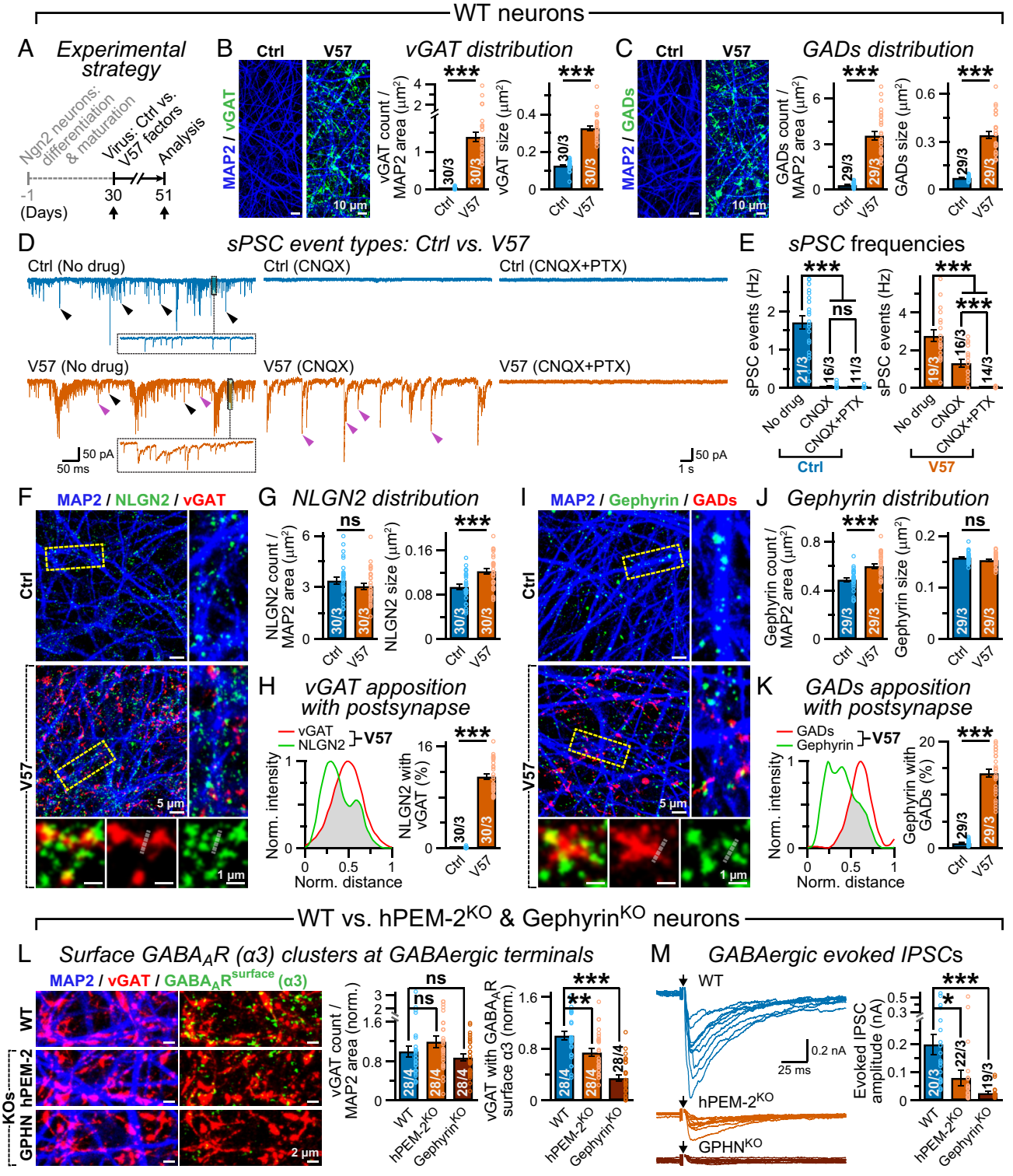

Fig. 6. Functional stimulation of GABAergic postsynapse by a delayed supply of presynaptic GABA. (*A*) Neurons were allowed to mature until day 30, then transduced with lentiviruses expressing V57 transgenes, and subsequently analyzed at day 51. (*B* and *C*) Representative images (*Left*) and average density or cluster size (*Right*) of vGAT (*B*) and GAD65/67 (*C*) puncta formed on MAP2-positive dendrites in control (Ctrl) vs. V57 conditions. (*D* and *E*) Sample traces of sPSC events (*D*) recorded from control (Ctrl, *Top*) vs. V57-transduced (*Bottom*) neurons, before (No drug, *Left*) and after acute bath-application of CNQX (*Middle*) or CNQX + PTX (*Right*); *Insets* = boxed regions magnified, arrowheads point at events with fast (black) vs. slow (purple) τ-decays. Average sPSC frequencies (*E*) before and after drug treatments. (*F*) Example images of Ctrl vs. V57-transduced neurons immunostained for MAP2, NLGN2, and vGAT, with boxed areas magnified (*Right*). For the V57 condition, merged signals (i.e., NLGN2 and vGAT) are further enlarged and depicted as individual channels with shared territories (*Bottom*). (*G*) Average density and size of NLGN2 clusters along MAP2-positive dendrites. (*H*) Spatial apposition of postsynaptic NLGN2 with presynaptic vGAT, depicted as superimposed intensity profiles (*Left*, gray area) from V57 conditions [dotted lines, panel (*F*) *Inset*]; percentages of NLGN2 signals (*Right*) colocalized with vGAT puncta in control vs. V57 conditions. (*I–K*) Same as (*F–H*), except for colocalizations between Gephyrin and GAD65/67. (*L*) WT vs. hPEM-2^{KO} and GPHN^{KO} neurons were transduced by V57 factors (day 30 to 51). Representative images (*Left*) of dendritic branches coimmunostained for MAP2, vGAT, and surface epitope of GABA$_A$R α3 (color-coded); average density of vGAT puncta and its relative apposition with α3 signals (*Right*). (*M*) Example recordings (*Left*; superimposed traces from 10 consecutive trials) and average peak amplitudes (*Right*) of inhibitory PSCs evoked by presynaptic stimulations (arrows, stimulus artifacts erased for clarity) in WT vs. hPEM-2^{KO} and GPHN^{KO} neurons at day 51. Summary graphs reflect means ± SEM. Statistics: Two-tailed, Student's *t* test, with ***$P < 0.005$; **$P < 0.01$; *$P < 0.05$; ns = not significant ($P > 0.05$).

Interestingly, despite a complete absence of GABA signaling, the Gephyrin scaffold remained physically isolated from its glutamatergic counterparts, e.g., Homer and PSD-95, even when they occasionally positioned adjacent to each other (Fig. 2 and *SI Appendix*, Fig. S2). Furthermore, within the same subsynaptic space, GABAergic postsynaptic CAM NLGN2 was preferentially captured by Gephyrin but not Homer clusters (Fig. 2). Therefore, the availability of separate presynapses with different neurotransmitter identities might not be absolutely necessary for the spatial segregation and compositional specificity of glutamatergic vs. GABAergic postsynapses, which instead could reflect an inherent mechanism defined by molecular interactions and/or intrinsic biophysical properties. For instance, liquid phase separation can directly contribute to a mutually exclusive organization of these two distinct postsynapses even during in vitro reconstitution, as demonstrated by a seminal study (50).

We noticed that genetic deletion of Gephyrin severely disrupted the submembrane accumulation of $GABA_A$Rs at both GABA-deficient and GABAergic human postsynapses (Figs. 4 and 6 and *SI Appendix*, Figs. S4 and S5). Hence, Gephyrin provides a crucial structural support for postsynaptic assembly, regardless of GABA signals. Of note, acute uncaging of GABA can directly promote Gephyrin aggregation, implying that activity-dependent pathways could further influence this process (26). In addition, earlier studies, including our own, have reported that chronic pharmacological inhibition of GABAergic activities can decrease, but does not completely abolish, subsynaptic accumulation of Gephyrin–$GABA_A$R (24, 25, 27, 51). We now illustrate that "orphan" GABAergic postsynapses developed without activity could be functionally stimulated post hoc by delayed supply of vesicular GABA, which further enhances Gephyrin clustering (Fig. 6). Therefore, GABA release can facilitate the maturation and/or long-term maintenance of existing postsynaptic structures (*SI Appendix*, Fig. S6).

We found strong evidence that GABAergic postsynapse assembly is critically regulated by a Rho-GEF factor Collybistin, also in a human cellular context. Isogenic KO of hPEM-2, i.e., human ortholog of Collybistin, produced a significant loss of Gephyrin scaffold and its association with NLGN2 and $GABA_A$Rs (Fig. 5). This provided another example of how intrinsic pathways can modulate the NLGN2–Gephyrin–$GABA_A$R complex, while operating independently of GABAergic activity. Even when GABA was later made available, hPEM-2^{KO} cells continued to elicit decreased amount of postsynaptic $GABA_A$Rs and diminished GABAergic synaptic strength (Fig. 6). Multiple loss-of-function mutations in hPEM-2 have been described in X-linked mental disorder, epilepsy, and hyperekplexia (52, 53). Our data indicate that dysregulation of GABAergic synapse assembly could be a probable pathogenic mechanism.

In the future, it would be important to explore how these self-organizing GABAergic postsynapses are able to recognize and appropriately align with GABA-less presynapses. Gephyrin itself is an intracellular protein that needs to receive spatial cues for correct subsynaptic trafficking. It is plausible that cis-interactions with certain CAMs including NLGN2, Slitrk3, etc., or even $GABA_A$R itself might enable Gephyrin monomers to initially localize underneath the postsynaptic membranes [(12, 20, 54); Fig. 3]. This nascent complex could consequently become enriched by Gephyrin's oligomerization properties and its binding affinities for other proteins, further modulated by Collybistin. Alternative splicing and posttranslational modifications of Gephyrin might also facilitate its assembly [(55, 56); Fig. 4, and *SI Appendix*, Fig. S4]. It was also unclear why GABA-free postsynapses failed to capture α2 containing $GABA_A$R or β-Dystroglycan (Figs. 1 and 2). Their synaptic association might require additional factors that were not addressed in our current study.

Summary Methods

All iPS cell culture methods and lentivirus production procedures were authorized by the institutional biosafety committee (IBC protocol # 19-059B) of Colorado State University. Primary glia extractions from the mouse brain were approved by the institutional animal care and use committee (IACUC protocol # 1482). For detailed Experimental Methods, see *SI Appendix*.

Data, Materials, and Software Availability. All study data are included in the article and/or *SI Appendix*. Data-points from each experiment are provided as color-matched symbols and presented along with corresponding average values.

ACKNOWLEDGMENTS. This work was supported by a start-up fund (Colorado State University) and a grant from the National Institute of Mental Health (R01-MH126017) to S.C. We thank Drs. Seonil Kim and James R. Bamburg, Colorado State University, for providing us with some experimental reagents. We also thank Drs. Robert E. Cohen and Tingting Yao, Colorado State University, for the access of Zeiss Airyscan microscope.

Author affiliations: [a]Department of Biochemistry and Molecular Biology, Colorado State University, Fort Collins, CO 80523; [b]Biological Sciences Division, University of Chicago, Chicago, IL 60637; [c]Molecular, Cellular and Integrated Neurosciences Program, Colorado State University, Fort Collins, CO 80523; and [d]Cell and Molecular Biology Program, Colorado State University, Fort Collins, CO 80523

Author contributions: S.C. designed research; E.C., O.B., C.D.S.P., and S.C. performed research; S.R.B. and S.C. contributed new reagents/analytic tools; E.C., O.B., S.R.B., N.H., C.H.K., and S.C. analyzed data; and S.C. wrote the paper.

1. S. K. Tyagarajan, J. M. Fritschy, Gephyrin: A master regulator of neuronal function? *Nat. Rev. Neurosci.* **15**, 141–156 (2014).
2. M. Kneussel *et al.*, Loss of postsynaptic GABA(A) receptor clustering in gephyrin-deficient mice. *J. Neurosci.* **19**, 9289–9297 (1999).
3. J. Mukherjee *et al.*, The residence time of GABA(A)Rs at inhibitory synapses is determined by direct binding of the receptor α1 subunit to gephyrin. *J. Neurosci.* **31**, 14677–14687 (2011).
4. V. Tretter *et al.*, The clustering of GABA(A) receptor subtypes at inhibitory synapses is facilitated via the direct binding of receptor alpha 2 subunits to gephyrin. *J. Neurosci.* **28**, 1356–1365 (2008).
5. V. Tretter *et al.*, Molecular basis of the γ-aminobutyric acid A receptor α3 subunit interaction with the clustering protein gephyrin. *J. Biol. Chem.* **286**, 37702–37711 (2011).
6. M. Kneussel *et al.*, Gephyrin-independent clustering of postsynaptic GABA(A) receptor subtypes. *Mol. Cell Neurosci.* **17**, 973–982 (2001).
7. M. Kneussel *et al.*, The gamma-aminobutyric acid type A receptor (GABAAR)-associated protein GABARAP interacts with gephyrin but is not involved in receptor anchoring at the synapse. *Proc. Natl. Acad. Sci. U.S.A.* **97**, 8594–8599 (2000).
8. J. C. Fuhrmann *et al.*, Gephyrin interacts with Dynein light chains 1 and 2, components of motor protein complexes. *J. Neurosci.* **22**, 5393–5402 (2002).
9. T. Giesemann *et al.*, Complex formation between the postsynaptic scaffolding protein gephyrin, profilin, and Mena: A possible link to the microfilament system. *J. Neurosci.* **23**, 8330–8339 (2003).
10. K. Harvey *et al.*, The GDP-GTP exchange factor collybistin: An essential determinant of neuronal gephyrin clustering. *J. Neurosci.* **24**, 5816–5826 (2004).
11. S. Kins, H. Betz, J. Kirsch, Collybistin, a newly identified brain-specific GEF, induces submembrane clustering of gephyrin. *Nat. Neurosci.* **3**, 22–29 (2000).
12. A. Poulopoulos *et al.*, Neuroligin 2 drives postsynaptic assembly at perisomatic inhibitory synapses through gephyrin and collybistin. *Neuron* **63**, 628–642 (2009).
13. T. Soykan *et al.*, A conformational switch in collybistin determines the differentiation of inhibitory postsynapses. *EMBO J.* **33**, 2113–2133 (2014).
14. R. Antonelli *et al.*, Pin1-dependent signalling negatively affects GABAergic transmission by modulating neuroligin2/gephyrin interaction. *Nat. Commun.* **5**, 5066 (2014).
15. A. Uezu *et al.*, Identification of an elaborate complex mediating postsynaptic inhibition. *Science* **353**, 1123–1129 (2016).
16. W. Yu *et al.*, Gephyrin clustering is required for the stability of GABAergic synapses. *Mol. Cell Neurosci.* **36**, 484–500 (2007).
17. S. Kim *et al.*, Impaired formation of high-order gephyrin oligomers underlies gephyrin dysfunction-associated pathologies. *Science* **24**, 102037 (2021).
18. S. Lévi *et al.*, Gephyrin is critical for glycine receptor clustering but not for the formation of functional GABAergic synapses in hippocampal neurons. *J. Neurosci.* **24**, 207–217 (2004).
19. H. J. Waldvogel *et al.*, Distribution of gephyrin in the human brain: An immunohistochemical analysis. *Neuroscience* **116**, 145–156 (2003).
20. J. Duan *et al.*, Genetic deletion of GABA. *Front Cell Neurosci.* **13**, 217 (2019).
21. T. Papadopoulos *et al.*, Impaired GABAergic transmission and altered hippocampal synaptic plasticity in collybistin-deficient mice. *EMBO J.* **26**, 3888–3899 (2007).

22. O. Babaev *et al.*, Neuroligin 2 deletion alters inhibitory synapse function and anxiety-associated neuronal activation in the amygdala. *Neuropharmacology* **100**, 56–65 (2016).
23. C. J. Wierenga, N. Becker, T. Bonhoeffer, GABAergic synapses are formed without the involvement of dendritic protrusions. *Nat. Neurosci.* **11**, 1044–1052 (2008).
24. V. Kilman, M. C. van Rossum, G. G. Turrigiano, Activity deprivation reduces miniature IPSC amplitude by decreasing the number of postsynaptic GABA(A) receptors clustered at neocortical synapses. *J. Neurosci.* **22**, 1328–1337 (2002).
25. B. Chattopadhyaya *et al.*, Experience and activity-dependent maturation of perisomatic GABAergic innervation in primary visual cortex during a postnatal critical period. *J. Neurosci.* **24**, 9598–9611 (2004).
26. W. C. Oh *et al.*, De novo synaptogenesis induced by GABA in the developing mouse cortex. *Science* **353**, 1037–1040 (2016).
27. S. R. Burlingham *et al.*, Induction of synapse formation by de novo neurotransmitter synthesis. *Nat. Commun.* **13**, 3060 (2022).
28. Y. Zhang *et al.*, Rapid single-step induction of functional neurons from human pluripotent stem cells. *Neuron* **78**, 785–798 (2013).
29. C. Wang *et al.*, Scalable production of iPSC-derived human neurons to identify tau-lowering compounds by high-content screening. *Stem Cell Rep.* **9**, 1221–1233 (2017).
30. S. Chanda *et al.*, Direct reprogramming of human neurons identifies MARCKSL1 as a pathogenic mediator of valproic acid-induced teratogenicity. *Cell Stem Cell* **25**, 103–119.e6 (2019).
31. S. Lévi *et al.*, Dystroglycan is selectively associated with inhibitory GABAergic synapses but is dispensable for their differentiation. *J. Neurosci.* **22**, 4274–4285 (2002).
32. J. H. Trotter *et al.*, A combinatorial code of neurexin-3 alternative splicing controls inhibitory synapses via a trans-synaptic dystroglycan signaling loop. *Nat. Commun.* **14**, 1771 (2023).
33. B. A. Barres *et al.*, Ion channel expression by white matter glia: The O-2A glial progenitor cell. *Neuron* **4**, 507–524 (1990).
34. S. Ochi *et al.*, Transient presence of GABA in astrocytes of the developing optic nerve. *Glia* **9**, 188–198 (1993).
35. C. J. Shatz, M. P. Stryker, Prenatal tetrodotoxin infusion blocks segregation of retinogeniculate afferents. *Science* **242**, 87–89 (1988).
36. B. Lendvai *et al.*, Experience-dependent plasticity of dendritic spines in the developing rat barrel cortex in vivo. *Nature* **404**, 876–881 (2000).
37. C. R. Yu *et al.*, Spontaneous neural activity is required for the establishment and maintenance of the olfactory sensory map. *Neuron* **42**, 553–566 (2004).
38. A. D. Huberman, C. M. Speer, B. Chapman, Spontaneous retinal activity mediates development of ocular dominance columns and binocular receptive fields in v1. *Neuron* **52**, 247–254 (2006).
39. M. Verhage *et al.*, Synaptic assembly of the brain in the absence of neurotransmitter secretion. *Science* **287**, 864–869 (2000).
40. F. Varoqueaux *et al.*, Total arrest of spontaneous and evoked synaptic transmission but normal synaptogenesis in the absence of Munc13-mediated vesicle priming. *Proc. Natl. Acad. Sci. U.S.A.* **99**, 9037–9042 (2002).
41. K. J. Harms, A. M. Craig, Synapse composition and organization following chronic activity blockade in cultured hippocampal neurons. *J. Comp. Neurol.* **490**, 72–84 (2005).
42. C. Imig *et al.*, The morphological and molecular nature of synaptic vesicle priming at presynaptic active zones. *Neuron* **84**, 416–431 (2014).
43. R. Sando *et al.*, Assembly of excitatory synapses in the absence of glutamatergic neurotransmission. *Neuron* **94**, 312–321.e3 (2017).
44. A. Sigler *et al.*, Formation and maintenance of functional spines in the absence of presynaptic glutamate release. *Neuron* **94**, 304–311.e4 (2017).
45. R. G. Held *et al.*, Synapse and active zone assembly in the absence of presynaptic Ca. *Neuron* **107**, 667–683.e9 (2020).
46. A. Rao, E. M. Cha, A. M. Craig, Mismatched appositions of presynaptic and postsynaptic components in isolated hippocampal neurons. *J. Neurosci.* **20**, 8344–8353 (2000).
47. C. Gally, J. L. Bessereau, GABA is dispensable for the formation of junctional GABA receptor clusters in *Caenorhabditis elegans*. *J. Neurosci.* **23**, 2591–2599 (2003).
48. H. J. Ramsay *et al.*, AMPA and GABAA receptor nanodomains assemble in the absence of synaptic neurotransmitter release. *Front Mol. Neurosci.* **16**, 1232795 (2023).
49. I. Brunig *et al.*, GABAergic terminals are required for postsynaptic clustering of dystrophin but not of GABA(A) receptors and gephyrin. *J. Neurosci.* **22**, 4805–4813 (2002).
50. M. Zeng *et al.*, Reconstituted postsynaptic density as a molecular platform for understanding synapse formation and plasticity. *Cell* **174**, 1172–1187.e16 (2018).
51. B. Chattopadhyaya *et al.*, GAD67-mediated GABA synthesis and signaling regulate inhibitory synaptic innervation in the visual cortex. *Neuron* **54**, 889–903 (2007).
52. K. Shimojima *et al.*, Loss-of-function mutation of collybistin is responsible for X-linked mental retardation associated with epilepsy. *J. Hum. Genet.* **56**, 561–565 (2011).
53. G. Lesca *et al.*, De novo Xq11.11 microdeletion including ARHGEF9 in a boy with mental retardation, epilepsy, macrosomia, and dysmorphic features. *Am. J. Med. Genet. A* **155A**, 1706–1711 (2011).
54. J. Li *et al.*, Molecular dissection of neuroligin 2 and Slitrk3 reveals an essential framework for GABAergic synapse development. *Neuron* **96**, 808–826.e8 (2017).
55. R. Dos Reis *et al.*, Complex regulation of Gephyrin splicing is a determinant of inhibitory postsynaptic diversity. *Nat. Commun.* **13**, 3507 (2022).
56. H. Ghosh *et al.*, Several posttranslational modifications act in concert to regulate gephyrin scaffolding and GABAergic transmission. *Nat. Commun.* **7**, 13365 (2016).